



# CATION HOMEOSTASIS AND TRANSPORT RELATED GENE MARKERS ARE DIFFERENTIALLY EXPRESSED IN PORCINE BUCCAL POUCH MUCOSAL CELLS DURING LONG-TERM CELLS PRIMARY CULTURE IN VITRO

Artur Bryja<sup>1</sup>, Marta Dyszkiewicz-Konwińska<sup>1,2</sup>, Maurycy Jankowski<sup>1</sup>, Piotr Celichowski<sup>3</sup>, Katarzyna Stefańska<sup>3</sup>, Agata Chamier-Gliszczyńska<sup>3</sup>, Blanka Borowiec<sup>1</sup>, Katarzyna Mehr<sup>4</sup>, Dorota Bukowska<sup>5</sup>, Paweł Antosik<sup>5</sup>, Małgorzata Bruska<sup>1</sup>, Maciej Zabel<sup>6,7</sup>, Michał Nowicki<sup>3</sup>, Bartosz Kempisty<sup>1,3,8</sup>

## Abstract

The mucous membrane is composed of two layers. The layer of stratified squamous epithelium and the underlying layer of the connective tissue. The epithelium is composed of keratinocytes that are in different stages of differentiation, depending on their localization. In our research, after isolation of primary *in vitro* cultured buccal pouch mucosal cells, we observed keratinocytes in various stages of differentiation and fibroblasts. These cells, depending on the ionic dynamics, may be subject to different morphological and biochemical transformations. Understanding the expression profile of the normal oral mucosal tissue is important for further research into the effects of biomaterials on the mucosal cells, their growth, proliferation, and differentiation.

The porcine buccal pouch mucosal cells were used in this study. The oral mucosa was separated surgically and isolated enzymatically. The cells were *in vitro* cultured for 30 days, and after each step of *in vitro* culture (7 days, 15 days, 30 days), samples were collected for isolation of total RNA. The gene expression profile was measured using Affymetrix microarray assays.

In results, we observed genes belonging to two ontology groups: cation homeostasis and cation transport. These genes were up-regulated after 7 days of *in vitro* culture as compared to down-regulation after 15 and 30 days of *in vitro* culture. These results suggested that dynamic growth, proliferation and cell adhesion are more intense in the first 7 days of *in vitro* culture. We also observed, for the first time, the expression of ATP13A3 in porcine oral mucosal cells.

**Running title:** Cation homeostasis and transport in porcine oral mucosal cells

**Keywords:** porcine oral mucosal cells, cations homeostasis, cations transport, ATP1B1, ATP13A3, STEAP

<sup>1</sup>Department of Anatomy, Poznan University of Medical Science, Poznań, Poland

<sup>2</sup>Department of Biomaterials and Experimental Dentistry, Poznan University of Medical Sciences, Poznań, Poland

<sup>3</sup>Department of Histology and Embryology, Poznan University of Medical Science, Poznań, Poland

<sup>4</sup>Department of Dental Prosthetics, Pomeranian Medical University in Szczecin, Szczecin, Poland

<sup>5</sup>Veterinary Center, Nicolaus Copernicus University in Toruń, Toruń, Poland

<sup>6</sup>Department of Histology and Embryology, Wrocław University of Medical Sciences, Wrocław, Poland

<sup>7</sup>Division of Anatomy and Histology, University of Zielona Góra, Zielona Góra, Poland

<sup>8</sup>Department of Obstetrics and Gynecology, University Hospital and Masaryk University, Brno, Czech Republic

\* **Correspondence:** bkempisty@ump.edu.pl

Full list of author information is available at the end of article

## Introduction

The oral cavity architecture is formed by mucous membrane covered by epithelium, basal lamina and deeper located connective tissue. It was shown in several studies that oral superficial cells layers undergo substantial morphological and biochemical modifications. The changes involve „morphological balance” between keratinocytes and fibroblasts that form the structure of mucosa, as well as changes in cellular metabolism as a direct response to oral cavity environment [1–3]. It is a fact that the oral mucous membrane is the first barrier to drug transport and delivery that significantly influences cell survival and/or apoptosis. The specificity of drug delivery belongs to the processes accompanied by blood vessel network development, blood circulation and the induction of angiogenesis. The compound systems of blood vessels network and pathways of drug transport are involved in the processes of drugs activity and administration [4]. The advanced experimental dentistry is based on the discovery of new pathways of drug activation and the possibility of application of several new biomaterials used in dentistry and/or implantology. It has been found that the application of new biomaterials is significantly associated with the biocompatibility of the material, which is regulated by activation of biochemical mechanisms that regulate several processes such as cell growth and development, proliferation, differentiation, and finally survival and/or apoptosis [5]. Moreover, the ability of oral tissues to form the blood vessel architecture and induce angiogenesis is strongly related to tissue regeneration and reconstruction after surgery or trauma. The plasticity of oral tissue and capability for the formation of new blood vessels belongs to the new strategies of human advanced experimental dentistry.

The *in vitro* culture of oral mucosal cells, particularly those of the buccal pouch, was presented in our previous studies for the first time [6]. We observed that the substantial increase of the real-time proliferation of porcine buccal pouch mucosal cells during long-term *in vitro* cultivation is accompanied by significant changes in gene expression profile responsible for cells growth, development and differentiation. However, the expression of genes regulating mucosal cell and tissue morphology was never investigated before.

## Material and Methods

### Animals

For this study, a total of 30 pubertal crossbred Landrace gilts bred on a commercial local farm were used. They had a mean age of 155 days (range 140 – 170 days), and the mean weight was 100 kg (95–120 kg). All of the animals were housed under identical conditions and fed the same forage (depending on age and reproductive status). The experiments were approved by the Local Ethical Committee of

the Poznan University of Life Sciences, Poland (permission no. 32/2012, 30.06.2012).

### Cell isolation and culture

After slaughter, samples of buccal pouch mucosa were obtained within 40 min and transported to the laboratory. The excised tissue was washed twice in Dulbecco's phosphate buffered saline (D-PBS; Sigma Aldrich, Madison, USA). The surface of the buccal pouch was surgically removed using sterile blades. The cell suspension obtained from this digestion was filtered through a mesh to remove non-dissociated tissue fragments and then incubated with 0.05% collagenase I (Sigma Aldrich, Madison, USA) for 40 min at 37 °C in a shaking water bath. Isolated cells were washed three times by centrifugation (10 min at 300 g) with Dulbecco's modified Eagle's medium (DMEM; Sigma Aldrich, Madison, USA) supplemented with gentamicin (20 µg/mL) and 0.1% BSA. The epidermal side of the mucosa was gently scraped with a scalpel to detach the keratinocytes. The resultant cell suspension was filtered through a 400-micron mesh and then washed three times by centrifugation (10 min at 300 g) with supplemented DMEM. The final cell pellet was resuspended in DMEM supplemented with 10% fetal calf serum (FCS; Sigma Aldrich, Madison, USA) and 100 U/ml penicillin G, 10 mg/ml streptomycin, and 0.25 µg/ml amphotericin B. Cell viability was 90 to 95% as determined by trypan blue staining (Sigma Aldrich, Madison, USA). The cells were cultured at 37 °C in a humidified atmosphere containing 5% CO<sub>2</sub>. Once the keratinocyte cultures attained 70–80% confluency, they were passaged by washing with PBS, digested with 0.025% trypsin/EDTA (Cascade Biologics, Portland, USA), neutralized by a 0.0125% trypsin inhibitor (Cascade Biologics, Portland, USA), centrifuged, and resuspended at a seeding density of 2x10<sup>4</sup> cells/cm<sup>2</sup>. The culture medium was changed every three days.

### Microarray expression analysis and statistics

Total RNA (100 ng) from each pooled sample was subjected to two rounds of sense cDNA amplification (Ambion® WT Expression Kit). The obtained cDNA was used for biotin labelling and fragmentation by Affymetrix GeneChip® WT Terminal Labeling and Hybridization (Affymetrix). Biotin-labelled fragments of cDNA (5.5 µg) were hybridized to the Affymetrix® Porcine Gene 1.1 ST Array Strip (48°C/20 h). Microarrays were then washed and stained according to the technical protocol using the Affymetrix GeneAtlas Fluidics Station. The array strips were scanned employing Imaging Station of the GeneAtlas System. Preliminary analysis of the scanned chips was performed using Affymetrix GeneAtlas™ Operating Software. The quality of gene expression data was confirmed according to the quality control criteria provided by the software.

The obtained CEL files were imported into downstream data analysis software.

All of the presented analyses and graphs were performed using Bioconductor and R programming languages. Each CEL file was merged with a description file. In order to correct background, normalize, and summarize results, we used the Robust Multi-array Averaging (RMA) algorithm. To determine the statistical significance of the analysed genes, moderated t-statistics from the empirical Bayes method were performed. The obtained p-value was corrected for multiple comparisons using Benjamini and Hochberg's false discovery rate. The selection of significantly altered genes was based on a p-value beneath 0.05 and expression higher than two-fold.

Differentially expressed genes were subjected selection by examination of genes involved in cation transport and homeostasis. The differentially expressed gene list was uploaded to DAVID software (Database for Annotation, Visualization and Integrated Discovery) [7], where genes belonging to "cation transport" and "cation homeostasis" gene ontology (GO) terms were obtained.

Interactions between differentially expressed genes/proteins belonging to the "cation transport" and "cation homeostasis" GO terms were investigated by STRING10 software (Search Tool for the Retrieval of Interacting Genes) [8]. The list of gene names was used as a query for an interaction prediction. The search criteria were based on co-occurrences of genes/proteins in scientific texts (text mining), co-expression, and experimentally observed interactions. The results of these analyses generated a gene/protein interaction network where the intensity of the edges reflected the strength of the interaction score.

In order to further investigate the changes in studied GO terms, we performed the z-score (the number of up-regulated genes minus the number of

down-regulated genes divided by the square root of the count) analysis using the GPlot package.

### Ethical approval

The research related to animal use has been complied with all the relevant national regulations and instructional policies for the care and use of animals. Bioethical Committee approval no. 32/2012.

### Results

Whole transcriptome profiling by Affymetrix microarray allows us to analyse the gene expression changes between 7, 15 and 30 days of buccal pouch mucosal cell culture. Using Affymetrix® Porcine Gene 1.1 ST Array Strip we examined the expression of 12257 transcripts. Genes with a fold change higher than abs (2) and with a corrected p-value lower than 0.05 were considered as differentially expressed. This set of genes consisted of 130 different transcripts.

DAVID (Database for Annotation, Visualization and Integrated Discovery) software was used for extraction of gene ontology biological process terms (GO-BP) that contain differently expressed transcripts. Up and down-regulated gene sets were subjected to DAVID searching separately and only gene sets where adj. p-value was lower than 0.05 were selected. The DAVID software analysis showed that the differentially expressed genes belonged to 56 Gene ontology groups. In this paper, we focused on "cation transport" and "cation homeostasis" GO BP terms. These sets of genes were subjected to hierarchical clusterization procedure and presented as heatmaps (**Fig. 1**). The gene symbols, fold changes of expression and corrected p values of that genes were shown in **table 1**. In order to further investigate the changes within chosen GO BP terms, we measured the enrichment levels of each selected GO BP terms. The enrichment levels were expressed as z-score and presented as circular visualization (**Fig. 2**).

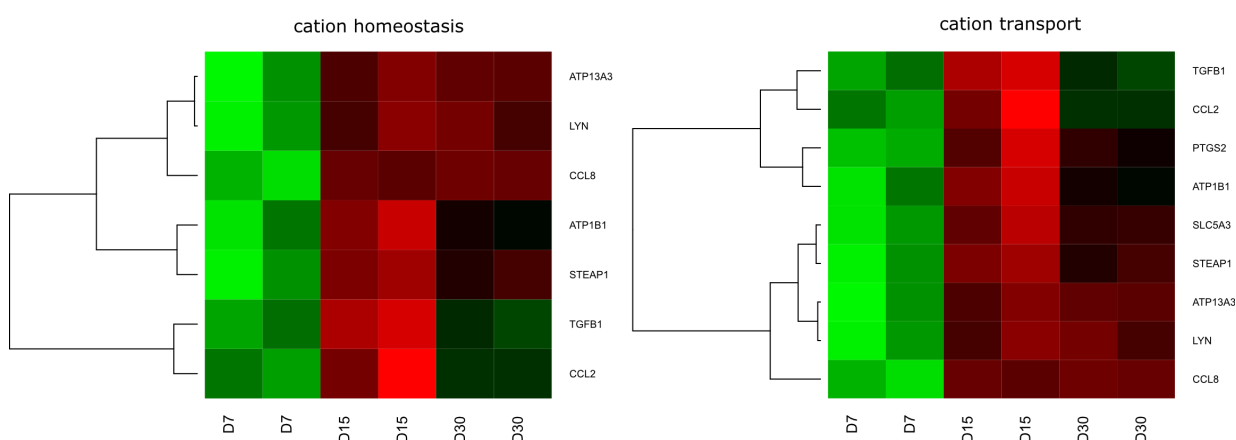


**Figure 1** Heat map representation of differentially expressed genes belonging to "cation transport" and "cation homeostasis" GO BP terms. Arbitrary signal intensity acquired from microarray analysis is represented by colours (green, higher; red, lower expression). Log2 signal intensity values for any single gene were resized to Row Z-Score scale (from -2, the lowest expression to +2, the highest expression for the single gene)

**TABLE 1** Gene symbols, fold changes in expression and corrected p values of studied genes

Gene symbol	FC D15/D7	FC D30/D7	FC D30/D15	P value D15/ D7	P value D30/ D7	P value D30/ D15
CCL8	0.109837	0.101557	0.924613	0.009909	0.002855	0.864829
PTGS2	0.176579	0.327797	1.856379	0.033272	0.086183	0.447703
SLC5A3	0.225224	0.33894	1.504902	0.028211	0.05553	0.540232
CCL2	0.254494	0.689284	2.708448	0.040744	0.404391	0.235089
ATP1B1	0.267104	0.497402	1.862204	0.031118	0.12303	0.326528
ATP13A3	0.279574	0.291783	1.04367	0.033845	0.040686	0.973114
LYN	0.396741	0.407409	1.026889	0.034636	0.042334	0.980695
STEAP1	0.425601	0.530046	1.245406	0.026836	0.044202	0.519251
TGFB1	0.443799	0.81545	1.837431	0.015016	0.216601	0.071989

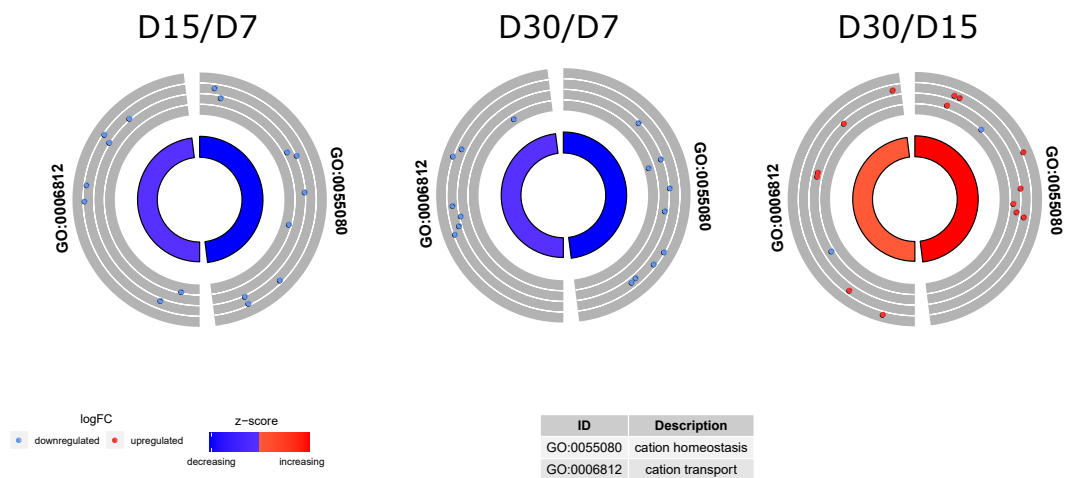


**Figure 2** The circular visualizations of the results of gene-annotation enrichment analysis between D15/D7, D30/D7 and D30/D15 respectively. The outer circles show a scatter plot for each term of the logFC of the assigned genes. Red circles display up-regulation and blue ones down-regulation. The inner circle is the representation of Z-score. The size and the colour of the bar correspond to the value of z-score

Moreover, genes that formed one particular GO group can also belong to other different GO term categories in Gene Ontology Database. For this reason, we explore the gene intersections between selected GO BP terms. The relation between those GO BP terms was presented as well chart (**Fig. 3**) as well as heatmap (**Fig. 4**).

STRING interaction network was generated between differentially expressed genes belonging to each of selected GO BP terms. Using such a prediction method provided us with the molecular interaction network formed between protein products of studied genes (**Fig. 5**).

**Discussion**

Cations and anions transport through the cell membrane and in the intracellular environment is important to the functioning of the cells. The cells isolated from the oral mucosa dynamically respond to a change in the concentration of cations in an environment when cultured *in vitro*. A good example of that is the influence of calcium ions on keratinocytes.

The mucous membrane is composed of two layers. The first layer of stratified squamous epithelium and the underlying layer of the connective tissue. The epithelium generally consists of keratinocytes. The basal layer consists of undifferentiated keratinocytes and when cells move from the basal layer to the superficial layer, they undergo various morphological and biochemical changes. These changes from undifferentiated to differentiated cells were observed during *in vitro* culture [9, 10]. The concentration of calcium cations is significant for keratinocyte survival. When *in vitro* content of Ca<sup>2+</sup> is at a low level, cells retain a basal phenotype, while the concentration of Ca<sup>2+</sup> at a high level contributes to keratinocyte differentiation [9]. Deyrieux and Wilson used HaCaT skin keratinocyte cell line in their study. When they transferred cells to low calcium medium (0.03 mM Ca<sup>2+</sup>), they observed that after 3 weeks the cells went back to the basal-like state. Later they analyzed cells cultured on a low calcium medium, after changing the medium to high calcium concentration (2.8 mM Ca<sup>2+</sup>). High calcium concen-

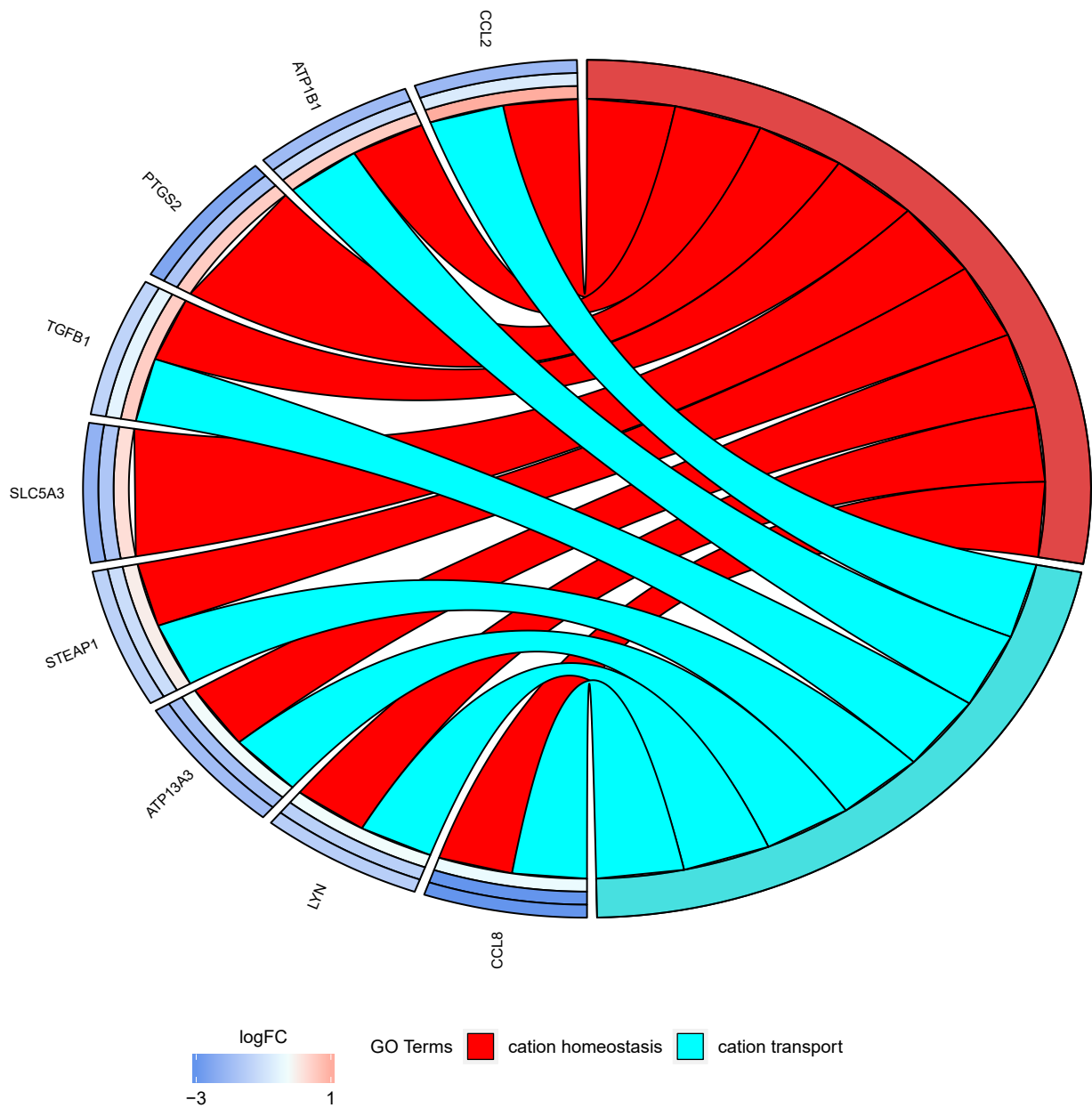


**Figure 3** The representation of the mutual relationship “cation transport” and “cation homeostasis” GO BP terms. The ribbons indicate which gene belongs to which categories. The genes were sorted by logFC from most to least changed gene. The logFC of these genes is represented by the inner circle, which represent the logFC between D15/D7, D30/D7 and D30/D15 respectively

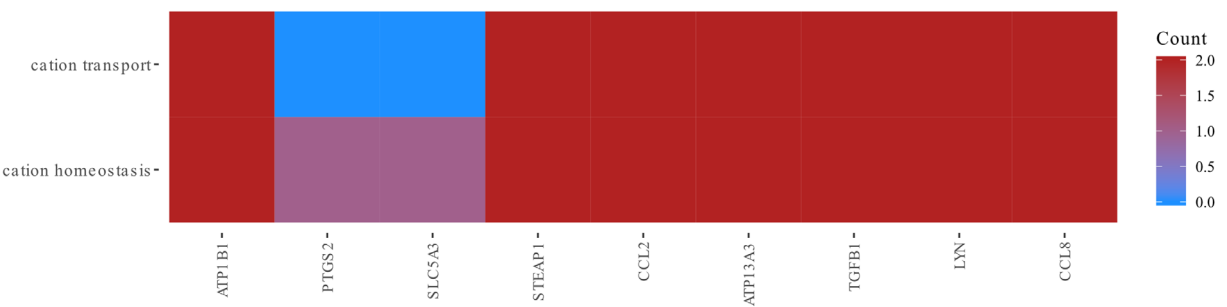


**Figure 4** Heatmap showing the gene occurrence between “cation transport” and “cation homeostasis” GO BP terms



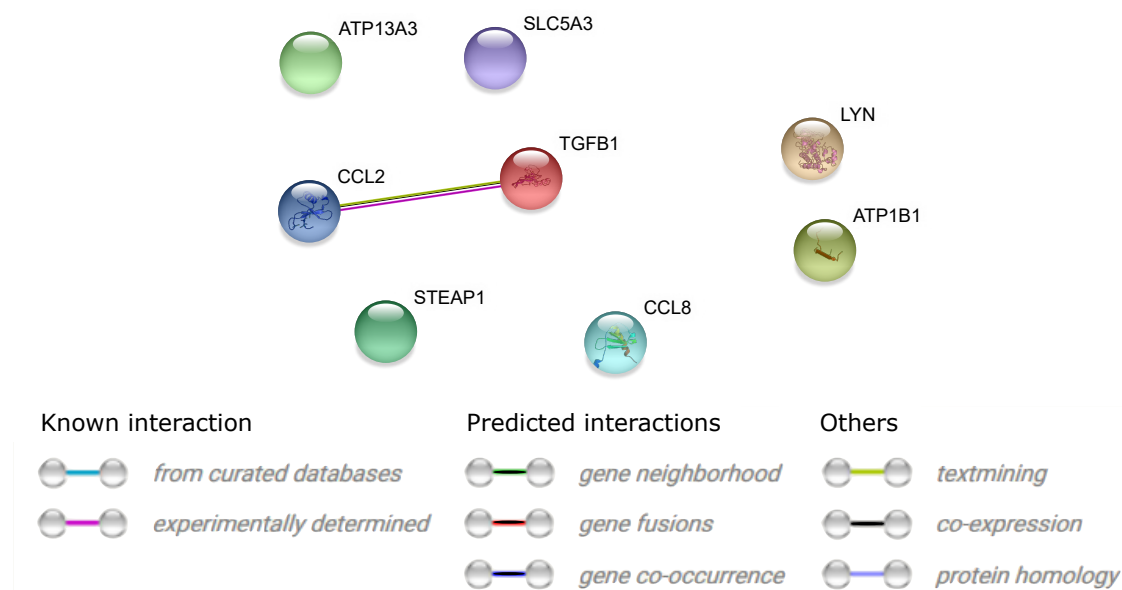


**Figure 5** STRING-generated interaction network among differentially expressed genes belonging to the “cation transport” and “cation homeostasis” GO BP terms. The intensity of the edges reflects the strength of the interaction score

tration induced differentiation of the HaCaT cells [9]. They also confirmed that the confluence of cells in culture affects the preservation of their basal or differentiated states. Hence, the confluence of keratinocyte cell cultures should be less than 85% [9].

In our *in vitro* culture, we have observed two types of cells: keratinocytes and fibroblasts. The fibroblasts form the feeder layer for keratinocytes, with both cell types growing on a regular DMEM culture medium. During long-term *in vitro* culture, keratinocytes undergo differentiation. It is also known that in primary *in vitro* culture, after induced differentiation, keratinocytes do not live long and cannot retain a basal phenotype [9].

In our research, we focused on the expression of mRNA of genes that belong to two ontology groups. The first, “cation homeostasis”, includes genes that were involved in the maintenance of an internal steady state of cations within a cell (GO:005580). The second group, “cation transport”, contains genes involved in the movement of cations in and out of, as well as between cells. (GO:0006812). From the analyzed genes: 6 belong to both ontology groups (ATP13A3, ATP1B1, CCL2, LYN, STEAP1, TGFB1), one belongs solely to cation homeostasis (CCL8), and two belong only to cation transport (PTGS2, SLC5A3). The expression of mRNA of the analyzed genes was the highest after 7 days of *in vitro* culture (IVC). The level of expression for most genes was reduced after 15 and 30 days of IVC. Only for two genes (TGFB1, CCL2), the expression level increased again after 30 days of IVC.

One of the important things for cell survival is the maintenance of the electrochemical potential on the cell membrane. Sodium/potassium-transporting ATPase beta 1 (ATP1B1) is a component of

the enzyme, which catalyzes the hydrolysis of ATP coupled with the exchange of  $\text{Na}^+$  and  $\text{K}^+$  ions across the plasma membrane. The  $\text{Na}^+/\text{K}^+$  ATPase is a plasma membrane pump which consists of alpha, beta and gamma subunit. The alpha subunit is a catalytic subunit. The beta subunit is responsible for the formation and integrity of the holoenzyme. Gamma subunit is a small hydrophobic polypeptide which is involved in modulation of pump function [11]. This pump is relevant for the maintenance of the intracellular ionic homeostasis. It is also known that the  $\text{Na}^+/\text{K}^+$  ATPase need  $\text{Mg}^{2+}$  that is not transported but essential for enzymatic activity [12].  $\text{Mg}^{2+}$  cations can bind to the cytoplasmic surface of the  $\text{Na}^+/\text{K}^+$  ATPase.  $\text{Mg}^{2+}$  ion reduces the local cation concentration in the electrolyte solution and at physiological concentrations can moderately alter the  $\text{Na}^+$ ,  $\text{K}^+$  and  $\text{H}^+$  concentrations. [12].

ATPase type 13A3 (ATP13A3) also belongs to the P-type ATPase family. This protein mediates transport of cations across the membrane. The faulty effect of ATP13A3 may lead to impaired ion homeostasis. There is little information describing the functions of this protein. The precise substrate specificity for ATP13A3 is unknown [13]. It is known that ATP13A3 plays a role in polyamine transport [14]. Graf et al. confirmed that ATP13A3 mRNA is expressed in primary cultured pulmonary artery smooth muscle cells and endothelial cells [13]. Loss of ATP13A3 inhibits proliferation and increases apoptosis of blood outgrowth endothelial cells (BOECs) [13]. Madan et al. analyzed the role of polyamine transport in pancreatic cancers [14]. The polyamines are required for cell growth and proliferation. At physiological pH, polyamines exist primarily as polycations and can be biosynthesized [14].

In our study, we observed a high-level of ATP1B1 and ATP13A3 expression in both ontology groups after 7 days of IVC. After 15 and 30 days of IVC, the level expression of ATP1B1 and ATP13A3 was lower than on 7 days of IVC. It was the first notice of ATP13A3 expression in epithelial cells. The high expression of ATP1B1 and ATP13A3 after 7 days of IVC is associated with cell growth and their proliferation. At a later time of IVC, the proliferation dynamics may be lower.

Another gene, for which we detected significant changes of expression in porcine buccal pouch mucosal cells in IVC, is six transmembrane epithelial antigen of the prostate 1 (STEAP1) which was primarily discovered in the prostate epithelium. In normal human tissues, it is expressed at a low level [15]. Mostly, it is overexpressed in numerous types of tumours in prostate cancer [16] and other human tumours such as colon, bladder and liver cancers [17]. Its physiological function is unclear. The level of STEAP1 expression is higher in the early stage than in the later stage of prostate cancer [17]. Ferrous STEAP1 can reduce metal ion complex of  $\text{Fe}^{3+}$  and  $\text{Cu}^{2+}$ . This protein plays a role of metal reductase and superoxide synthase [17]. Challita-Eid et al. described that STEAP1 plays a role as an intercellular communication protein and may promote tumour growth *in vivo* [18]. The secondary structure of STEAP1 may predispose it to be a protein transporter or may affect intercellular communication by altering intracellular ion concentrations, which in turn regulate gap or adherence junction activity [18]. When we compared this information's with our results, we may conclude that STEAP1 may be important for metal ion metabolism which is a confirmation of work presented by Kim et al.

Vaghjiani et al. investigated the expression of STEAP1 and STEAP2 in murine and human mesenchymal stem cells (MSCs). When they conducted the depletion of STEAP1 in human MSCs using RNAi, the cell adhesion to tissue culture plastic has been decreased [19].

We observed higher expression of STEAP1 after 7 days of IVC and decreased expression in the next days of IVC. This result may confirm the conclusions described by Vaghjiani et al. [19]. In the early stages of IVC, cells undergo a period of adaptation to new environmental conditions and in this time the process of cell adhesion to the culture dish is extremely important.

In conclusion, we observed increased gene expression in the initial phase of IVC. In subsequent time intervals, the expression of most genes was lower compared to day 7. Increased expression of ATP1B1, ATP13A3 and STEAP1 may indicate cells adhesion process, extracellular matrix formation, and intercellular connection creation.

## Acknowledgements

This publication and its results are an outcome of a cooperation between Poznan University of Medical Sciences (Poznań, Poland) and Polish Ministry of Science and Higher Education, with Institute of Advanced Sciences Sp. z o.o. (Poznań, Poland), as a part of the "Professional PhD" programme.

## Corresponding author

Bartosz Kempisty PhD, Department of Histology and Embryology, Department of Anatomy, Poznan University of Medical Sciences, 6 Święcickiego St., 60-781 Poznań, Poland Tel./Fax: +48 61 8546418 / +48 61 8546440, e-mail: bkempisty@ump.edu.pl.

## Conflict of interest statement

The authors declare they have no conflict of interest.

## References

- Chen J, Ahmad R, Li W, Swain M, Li Q. Biomechanics of oral mucosa. *J R Soc Interface*. 2015;12(109); DOI:10.1098/rsif.2015.0325.
- Agrawal U, Rai H, Jain AK. Morphological and ultrastructural characteristics of extracellular matrix changes in oral squamous cell carcinoma. *Ind J Dent Res*. 2011;22(1):16; DOI:10.4103/0970-9290.79968.
- Naumova EA, Dierkes T, Sprang J, Arnold WH. The oral mucosal surface and blood vessels. *Head Face Med*. 2013;9:8; DOI:10.1186/1746-160X-9-8.
- Zhang H, Zhang J, Streisand JB. Oral mucosal drug delivery: clinical pharmacokinetics and therapeutic applications. *Clin Pharmacokinet*. 2002;41(9):661–80; DOI:10.2165/00003088-200241090-00003.
- Jansen RG, van Kuppevelt TH, Daamen WF, Kuijpers-Jagtman AM, Von den Hoff, Johannes W. Tissue reactions to collagen scaffolds in the oral mucosa and skin of rats: environmental and mechanical factors. *Arch Oral Biol*. 2008;53(4):376–87; DOI:10.1016/j.archoralbio.2007.11.003.
- Dyszkiewicz-Konwińska M, Nawrocki M, Huang Y, Bryja A, Celichowski P, Jankowski M, Błochowiak K, Mehr K, Bruska M, Nowicki M, Zabel M, Kempisty B. New gene markers for metabolic processes and homeostasis in porcine buccal pouch mucosa during cells long term-cultivation - a primary culture approach. *IJMS*. 2018;19(4):1027; DOI:10.3390/ijms19041027.
- Huang DW, Sherman BT, Tan Q, Collins JR, Alvord WG, Roayaei J, Stephens R, Baseler MW, Lane HC, Lempicki RA. The DAVID Gene Functional Classification Tool: a novel biological module-centric algorithm to functionally analyze large gene lists. *Genome Biol*. 2007;8(9):R183; DOI:10.1186/gb-2007-8-9-r183.
- Mering C von, Jensen LJ, Snel B, Hooper SD, Krupp M, Foglierini M, Joutfré N, Huynen MA, Bork P. STRING: known and predicted protein-protein associations, integrated and transferred across organisms. *Nucleic Acids Res*. 2005;33(Database issue):D433–7; DOI:10.1093/nar/gki005.
- Deyrieux AF, Wilson VG. In vitro culture conditions to study keratinocyte differentiation using the HaCaT cell line. *Cytotechnology*. 2007;54(2):77–83; DOI:10.1007/s10616-007-9076-1.
- Parikh N, Nagarajan P, Sei-ichi M, Sinha S, Garrett-Sinha LA. Isolation and characterization of an immortalized oral keratinocyte cell line of mouse origin. *Arch Oral Biol*. 2008;53(11):1091–100; DOI:10.1016/j.archoralbio.2008.07.002.
- Li Y, Yang J, Li S, Zhang J, Zheng J, Hou W, Zhao H, Guo Y, Liu X, Dou K, Situ Z, Yao L. N-myc downstream-regulated gene 2, a novel estrogen-targeted gene, is involved in the regulation of  $\text{Na}^+/\text{K}^+$ -ATPase. *J Biol Chem*. 2011;286(37):32289–99; DOI:10.1074/jbc.M111.247825.
- Apell H-J, Hitzler T, Schreiber G. Modulation of the  $\text{Na}_2\text{K-ATPase}$  by Magnesium Ions. *Biochemistry*. 2017;56(7):1005–16; DOI:10.1021/acs.biochem.6b01243.
- Graf S, Haimel M, Bleda M, Hadinnapola C, Southgate L, Li W, Hodgson J, Liu B, Salmon RM, Southwood M, Machado RD, Martin JM, Treacy CM, Yates K, Daugherty LC, Shamardina O, Whitehorn D, Holden S, Aldred M, Bogaard HJ, Church C, Coghlan G, Condliffe R, Corris PA, Danesino C, Eyries M, Gall H, Ghio S, Ghofrani H-A, Gibbs JSR, Girerd B, Houweling AC, Howard L, Humbert M, Kiely DG, Kovacs G, MacKenzie Ross RV, Moledina S, Montani D, Newnham M, Olschewski A, Olschewski H, Peacock AJ, Pepke-Zaba J, Prokopenko I, Rhodes CJ, Scelsi L, Seeger W, Soubrier F, Stein DF, Suntharalingam J, Swietlik EM, Toshner MR, van Heel DA, Vonk Noordegraaf A, Waisfisz Q, Wharton J, Wort SJ, Ouwehand WH, Soranzo N, Lawrie A, Upton PD, Wilkins MR, Trembath RC, Morrell NW. Identification of rare sequence variation underlying heritable pulmonary arterial hypertension. *Nat Commun*. 2018;9(1):1416; DOI:10.1038/s41467-018-03672-4.

14. Madan M, Patel A, Skrubber K, Geerts D, Altomare DA, Iv OP. ATP13A3 and caveolin-1 as potential biomarkers for difluoromethylornithine-based therapies in pancreatic cancers. *Am J Cancer Res.* 2016;6(6):1231–52.
15. Esmaeili S-A, Nejatollahi F, Sahebkar A. Inhibition of intercellular communication between prostate cancer cells by a specific anti-STEAP-1 single chain antibody. *Anticancer Agents Med Chem.* 2017; DOI:10.2174/1871520618666171208092115.
16. Gomes IM, Rocha SM, Gaspar C, Alvelos MI, Santos CR, Socorro S, Maia CJ. Knockdown of STEAP1 inhibits cell growth and induces apoptosis in LNCaP prostate cancer cells counteracting the effect of androgens. *Med Oncol.* 2018;35(3):40; DOI:10.1007/s12032-018-1100-0.
17. Kim K, Mitra S, Wu G, Berka V, Song J, Yu Y, Poget S, Wang D-N, Tsai A-L, Zhou M. Six-Transmembrane Epithelial Antigen of Prostate 1 (STEAP1) has a single b heme and is capable of reducing metal ion complexes and oxygen. *Biochemistry.* 2016;55(48):6673–84; DOI:10.1021/acs.biochem.6b00610.
18. Challita-Eid PM, Morrison K, Etessami S, An Z, Morrison KJ, Perez-Villar JJ, Raitano AB, Jia X-C, Gudas JM, Kanner SB, Jakobovits A. Monoclonal antibodies to six-transmembrane epithelial antigen of the prostate-1 inhibit intercellular communication in vitro and growth of human tumor xenografts in vivo. *Cancer Res.* 2007;67(12):5798–805; DOI:10.1158/0008-5472.CAN-06-3849.
19. Vaghjiani RJ, Talma S, Murphy CL. Six-transmembrane epithelial antigen of the prostate (STEAP1 and STEAP2)-differentially expressed by murine and human mesenchymal stem cells. *Tissue Eng Part A.* 2009;15(8):2073–83; DOI:10.1089/ten.tea.2008.0519.